Defining the challenges of Li extraction with olivine host: the roles of competitor and spectator ions

Gangbin Yan[1], Mingzhan Wang[1], Grant T. Hill[1], Siqi Zou[1] and Chong Liu[1, *]

[1]Pritzker School of Molecular Engineering, University of Chicago, Chicago, IL 60637, USA
[*]Correspondence: chongliu@uchicago.edu

Table of Contents

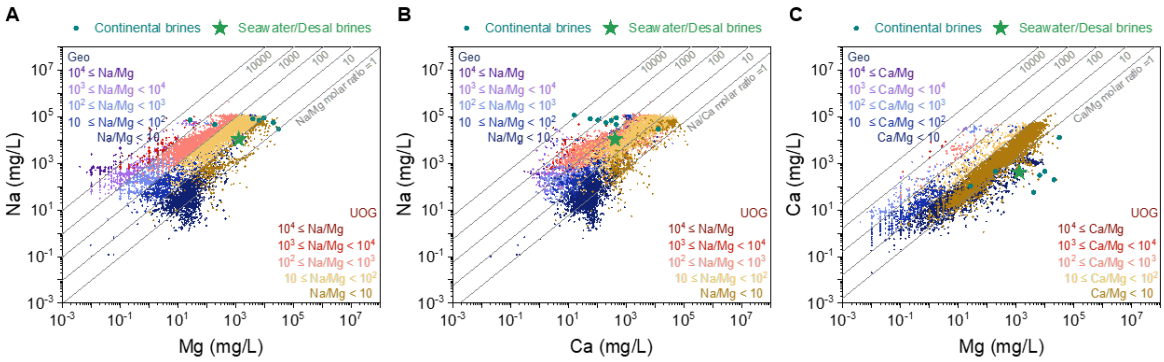

Fig. S1. (*A*) Na-Mg ion concentration. **(*B*)** Na-Ca ion concentration. **(*C*)** Ca-Mg ion concentration in continental brines, US Geo/UOG, and seawater/Desal water. Equimolar ratio reference lines are also labeled in grey.

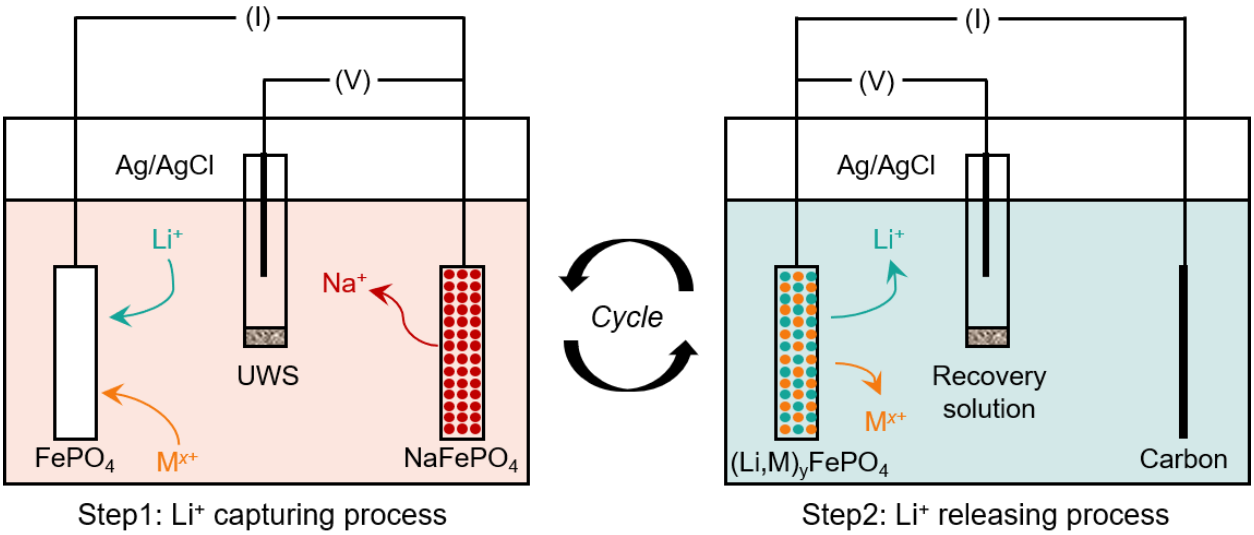

Fig. S2. Typical electrochemical Li^+ extraction cycle from UWS, using $FePO_4$ hosts as an example. (M^{x+} represents Na^+, K^+, Mg^{2+}, Ca^{2+}, or their combinations)

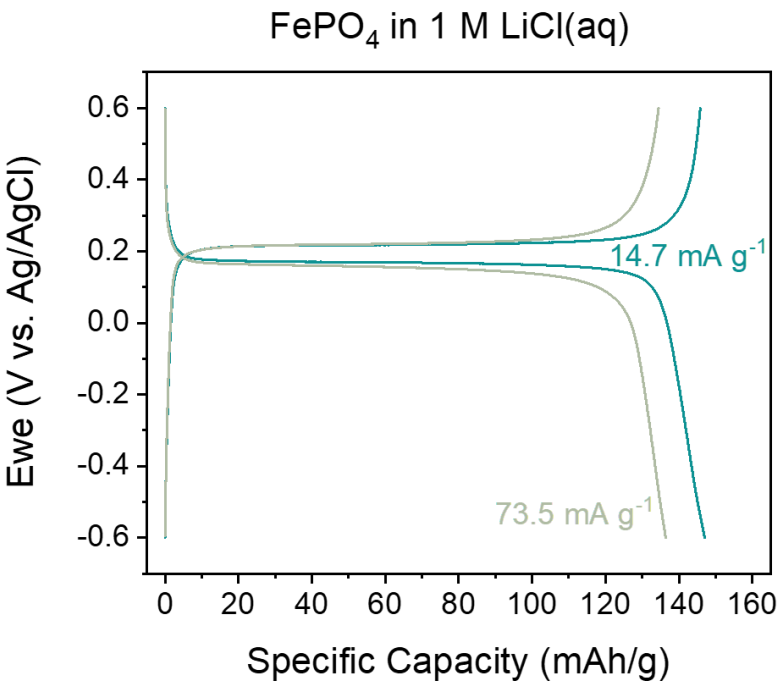

Fig. S3. Electrochemical cycling of the $FePO_4$ electrodes in 1 M LiCl aqueous solution under different current densities/C rates. 147 mA/g equals 1C.

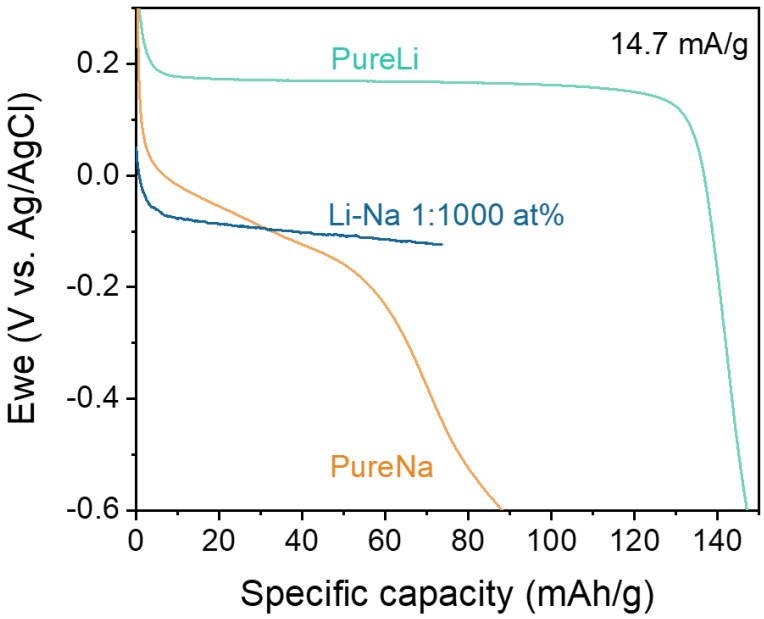

Fig. S4. Electrochemical intercalation curves of $FePO_4$ electrodes in 1 M LiCl(aq), 1 M NaCl(aq), and 1: 1000 Li-Na(aq) solutions under 14.7 mA/g (0.1C).

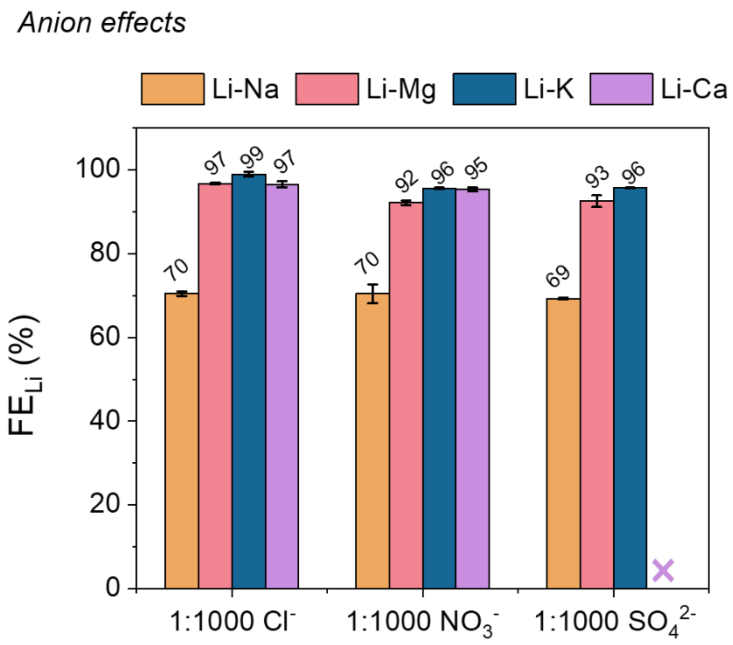

Fig. S5. Faraday efficiency of Li extraction in binary (Li-Na/Mg/K/Ca) solutions with different anions (Cl^-, NO_3^-, and SO_4^{2-}). The molar ratios of cations is fixed at 1: 1000 Li-M1 and the extraction C rate is 0.1C. (Error bars representing the standard deviation of three replicate measurements; [Li^+] is kept at 1 mM; Since $CaSO_4$ is poorly soluble in water, we didn't test the Li-Ca selectivity with SO_4^{2-} being the anions.)

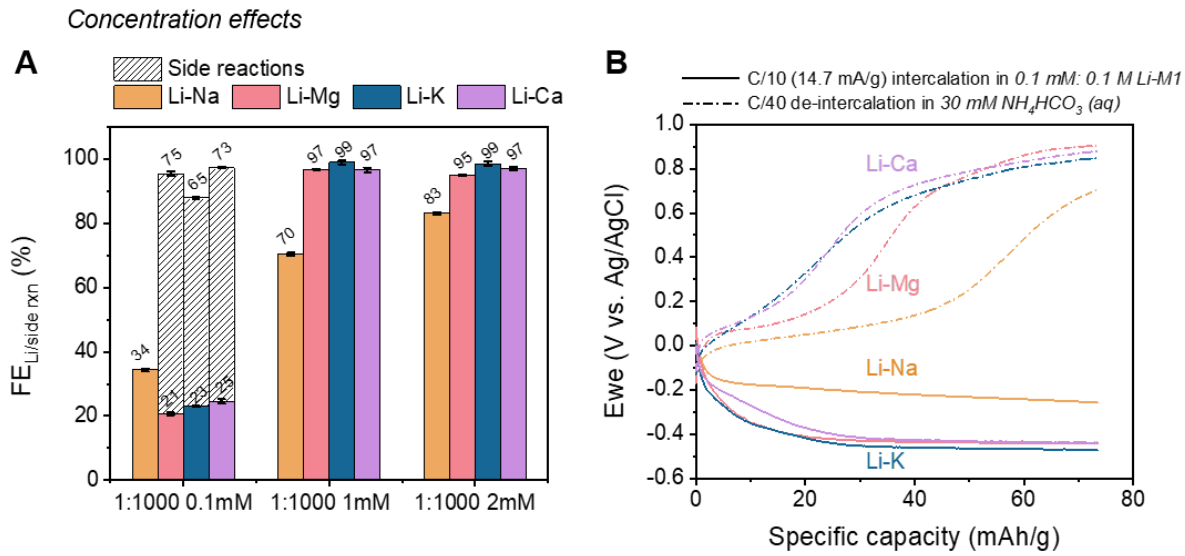

Fig. S6. Performance in binary (Li-M1) solutions with different total concentrations. (*A*) Faraday efficiency of Li and potential side reactions in binary (Li-Na/Mg/K/Ca) solutions with a fixed 1: 1000 molar ratio but different concentrations ($[Li^+]$ = 0.1 mM, 1 mM, and 2 mM; Error bars representing the standard deviation of three replicate measurements). **(*B*)** Chronopotentiometry (CP) 0.1C (14.7 mA/g) intercalation curves in *0.1 mM: 0.1 M Li-M1* aqueous solution and corresponding C/40 (3.675 mA/g) de-intercalation curves in *30 mM NH_4HCO_3* recovery solution, with the use of 50% of the total capacity (73.5 mAh/g).

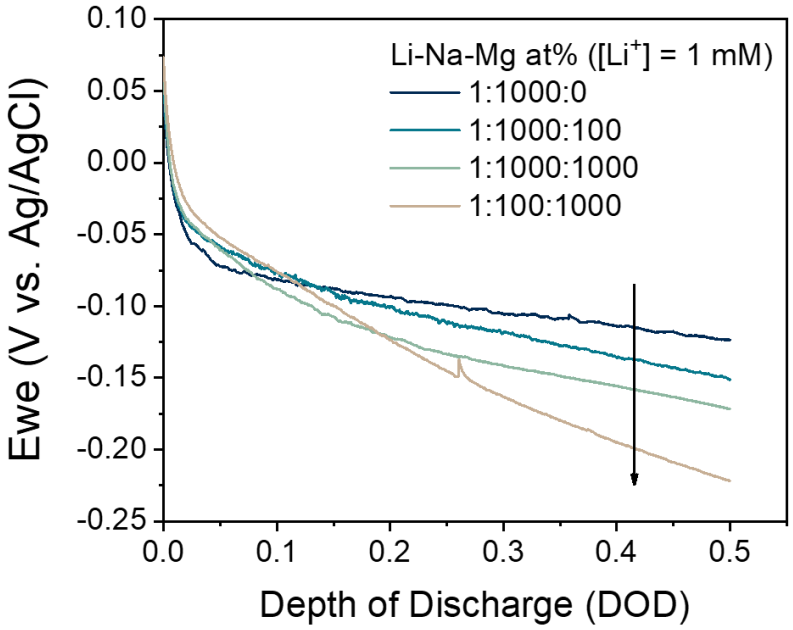

Fig. S7. Chronopotentiometry (CP) intercalation curves in Li-Na-Mg ternary solutions with different molar ratios under 0.1C ([Li^+] is kept at 1 mM).

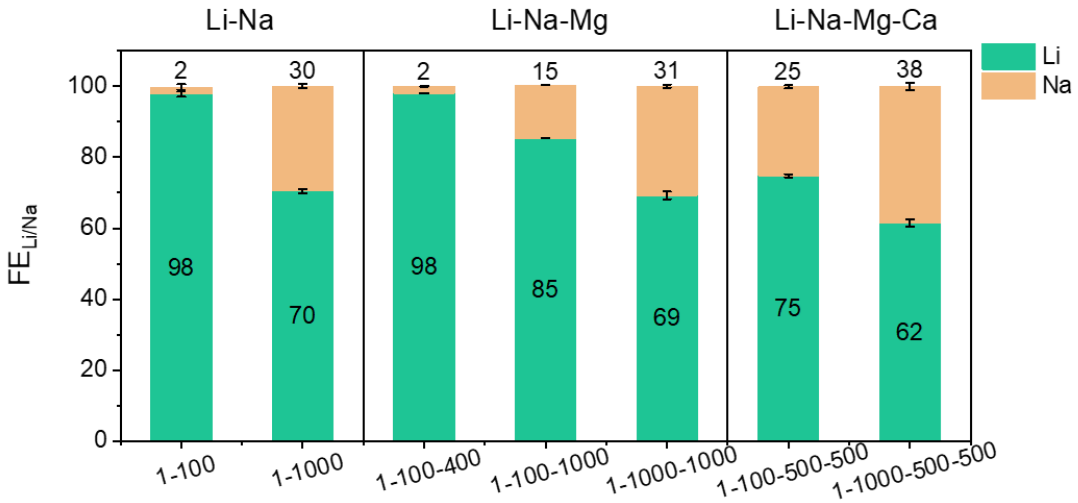

Fig. S8. Faraday efficiency of Li extraction in binary (Li-Na), ternary (Li-Na-Mg), and quaternary (Li-Na-Mg-Ca) solutions with different molar ratios under 0.1C extraction C rate. (Error bars representing the standard deviation of three replicate measurements; [Li^+] is kept at 1 mM.)

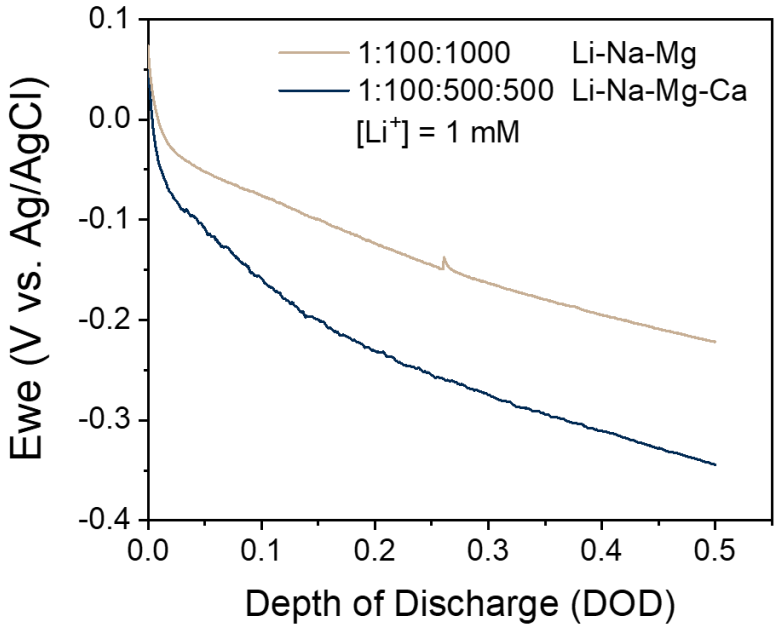

Fig. S9. Chronopotentiometry (CP) intercalation curves in 1: 100: 1000 Li-Na-Mg ternary solution and 1: 100: 500: 500 Li-Na-Mg-Ca quaternary solution under 0.1C ([Li^+] is kept at 1 mM).

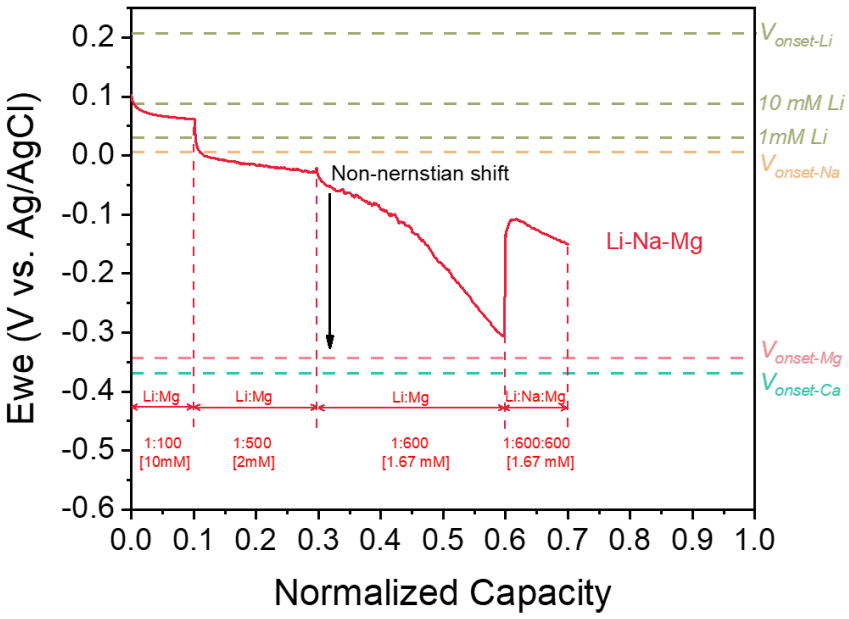

Fig. S10. Step-concentration chronopotentiometry (Stepconc CP) tests in Li-Na-Mg ternary system, with the final step changing from 1: 600 Li-Mg to 1: 600: 600 Li-Na-Mg ([Mg^{2+}] is kept at 1 M; $V_{onset\text{-}Li/Na/Mg/Ca}$ are acquired from the starting potential of the cathodic current peak during CV scan in Fig. 3*A*; *10 mM* and *1 mM* Li denote the Nernstian potential shift corrected by Li concentration change).

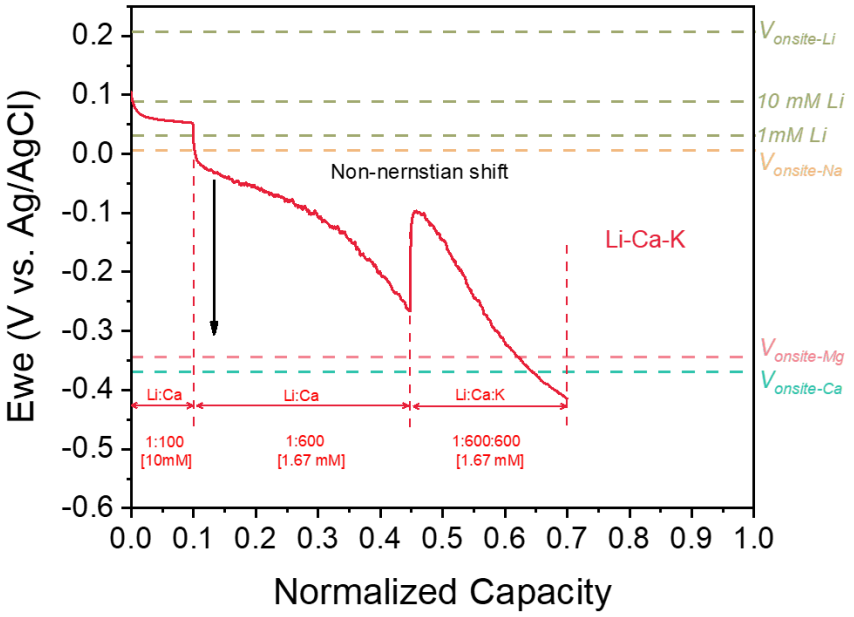

Fig. S11. Step-concentration chronopotentiometry (Stepconc CP) tests in Li-Ca-K ternary system, with the final step changing from 1: 600 Li-Ca to 1: 600: 600 Li-Ca-K ([Ca^{2+}] is kept at 1 M; $V_{onset\text{-}Li/Na/Mg/Ca}$ are acquired from the starting potential of the cathodic current peak during CV scan in Fig. 3*A*; *10 mM* and *1 mM* Li denote the Nernstian potential shift corrected by Li concentration change).

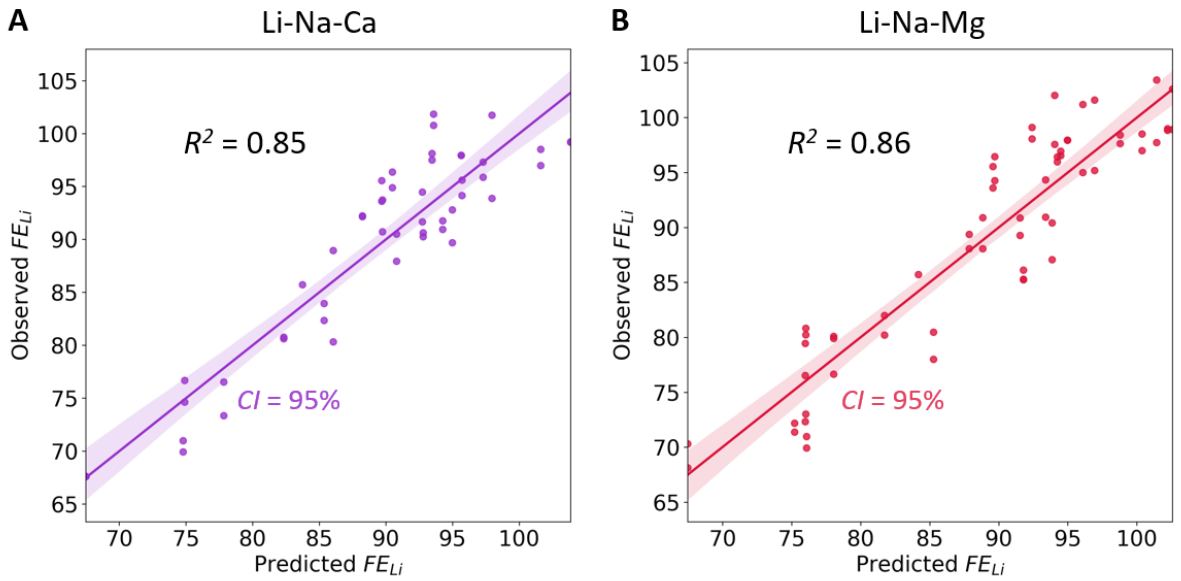

Fig. S12. Observed versus predicted FE_{Li} in (*A*) Li-Na-Ca ternary solutions and (***B***) Li-Na-Mg ternary solutions with the corresponding R^2 value. (The shaded areas representing the 95% confidence intervals).

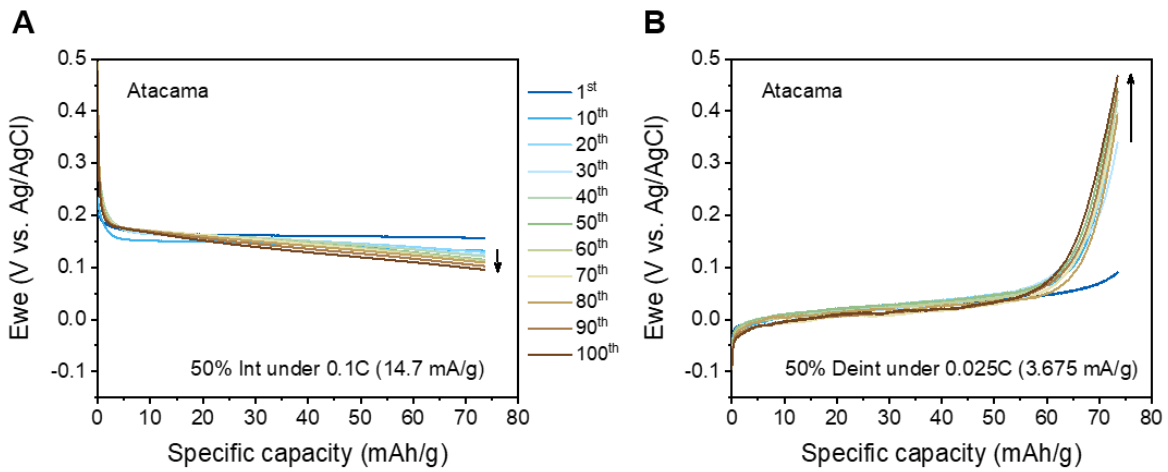

Fig. S13. Constant current (*A*) intercalation (14.7 mA/g) in simulated Atacama brine and (*B*) deintercalation (3.675 mA/g) in 30 mM NH_4HCO_3 (aq) recovery solution.

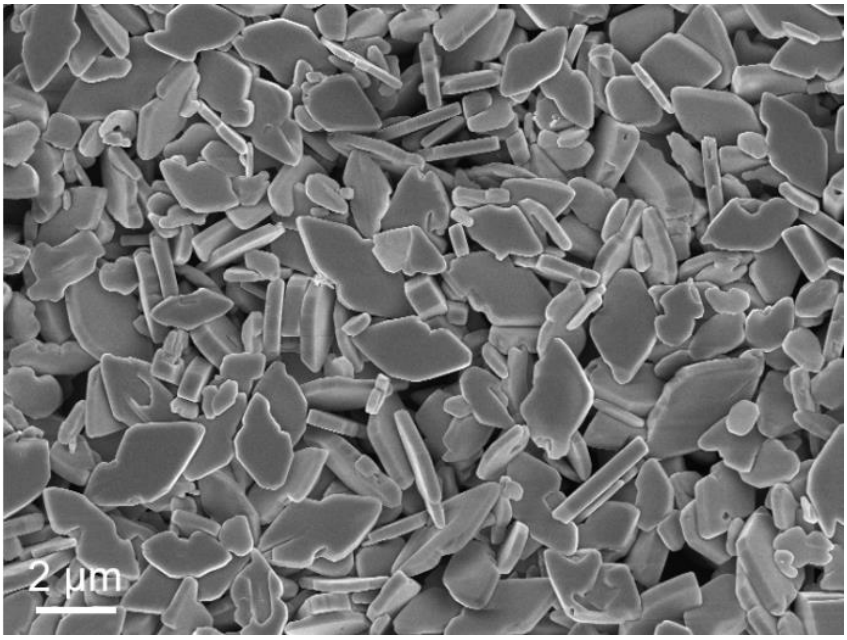

Fig. S14. SEM image of synthesized micro-sized $LiFePO_4$ platelet particles.

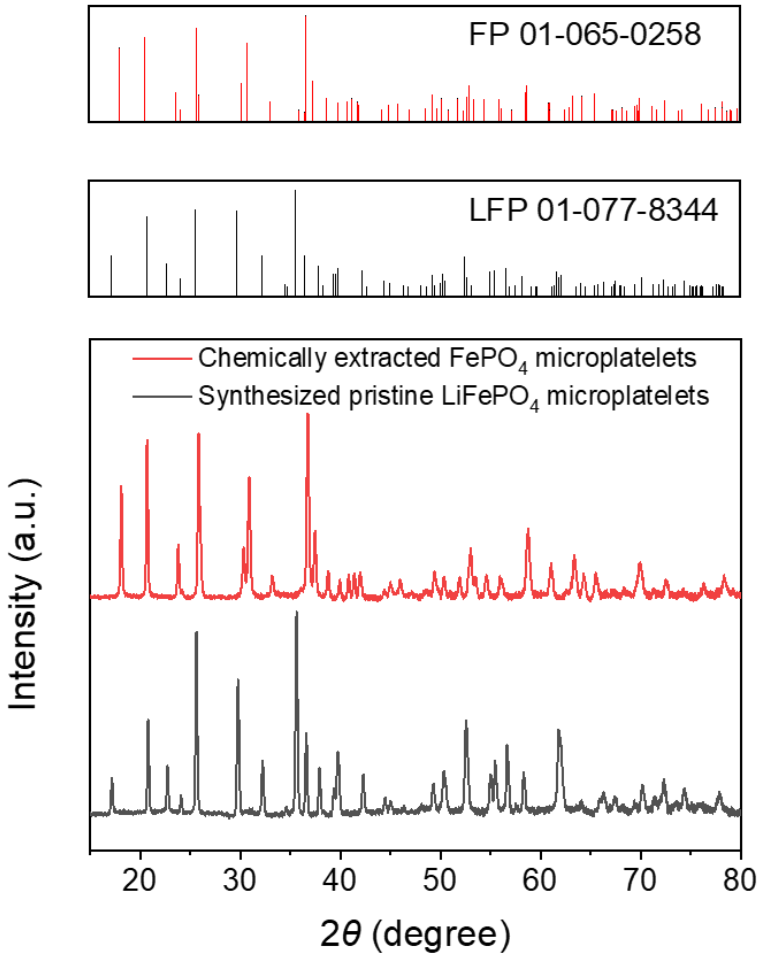

Fig. S15. XRD patterns of synthesized $LiFePO_4$ microplatelets and chemically extracted $FePO_4$ microplatelets with corresponding standard PDF cards (Olivine $LiFePO_4$ phase: 01-077-8344; Olivine $FePO_4$ phase: 01-065-0258).

Table S1. Properties of the main ions, including ionic/hydrated radii[1], and hydration enthalpy[2].

Ion	Li^+	Na^+	K^+	Mg^{2+}	Ca^{2+}
Ionic radii (Å)	0.60	0.95	1.33	0.65	0.99
Hydrated radii (Å)	3.82	3.58	3.31	4.28	4.12
Hydration Enthalpy (kJ/mol)	-515	-409	-322	-1921	-1577

Table S2. Migration barriers for cations in charged hosts and vacancy in discharged hosts[3-5].

Ion		Li^+	Na^+	K^+	Mg^{2+}	Ca^{2+}
Migration barriers (meV)	Cation migration	170	290	N.A.	680	572
	Vacancy migration	282	375		1158	930

Table S3. Voltages for the lithiation, sodiation or magnesiation of olivine $FePO_4$ compounds[6,7].

	Li	Na	Mg
Voltage (V vs. Ag/AgCl)	0.213	0.103	-0.167

Table S4. Continental brine compositions[8].

Continental brines	Li (mg/L)	Na (mg/L)	Mg (mg/L)	K (mg/L)	Ca (mg/L)
Salar de Atacama, Chile	1,570	91,000	9,650	23,600	450
Dead Sea, Israel	12	30,100	30,900	5,600	12,900
Taijinaier, China	310	56,300	20,200	4,400	200
Clayton Valley, USA	163	46,900	190	4,000	450
Searles Lake, USA	54	118,000	/	25,300	16
Bonneville, USA	57	83,000	4,000	5,000	57
Salton Sea, USA*	10,0 ~ 40,0	50,000 ~ 70,000	700 ~ 5,700	13,000 ~ 24,000	22,600 ~ 39,000
Great Salt Lake, USA*	18	37,000 ~ 87,000	5,000 ~ 9,700	2,600 ~ 7,200	260 ~ 360
Hombre Muerto, Argentina*	680 ~ 1,210	99,000 ~ 103,000	180 ~ 1,400	2,400 ~ 9,700	190 ~ 900
Salar de Uyuni, Bolivia	321	70,600	6,500	11,700	306
Sua Pan, India	20	60,000	/	2,000	/
Zabuye, China	489	72,900	26	16,600	106
		Li: Na (molar ratio)	**Li: Mg (molar ratio)**	**Li: K (molar ratio)**	**Li: Ca (molar ratio)**
Salar de Atacama, Chile		1: 18	1: 1.79	1: 2.7	1: 0.05
Dead Sea, Israel		1: 763	1: 751	1: 84	1: 188
Taijinaier, China		1: 55	1: 19	1: 3	1: 0.113
Clayton Valley, USA		1: 88	1: 0.34	1: 4.4	1: 0.48
Searles Lake, USA		1: 665	/	1: 84	1: 0.052
Bonneville, USA		1: 443	1: 20	1: 16	1: 0.175
Salton Sea, USA		1: 213 ~ 1: 38	1: 17 ~ 1: 0.51	1: 43 ~ 1: 6	1: 68.25 ~ 1: 10
Great Salt Lake, USA		1: 1,471 ~ 1: 626	1: 157 ~ 1: 81	1: 72 ~ 1: 26	1: 3.5 ~ 1: 2.5
Hombre Muerto, Argentina		1: 46 ~ 1: 25	1: 0.6 ~ 1: 0.043	1: 3 ~ 1: 0.356	1: 0.23 ~ 1: 0.03
Salar de Uyuni, Bolivia		1: 67	1: 5.9	1: 6.5	1: 0.167
Sua Pan, India		1: 913	/	1: 18	/
Zabuye, China		1: 45	1: 0.0155	1: 6	1: 0.04

(Notes: 1. Only cations with high concentrations are provided in addition to Li^+; 2. * denotes arithmetic mean values of the concentrations are used to be plotted in Fig. 5)

Supplementary References

1 Nightingale, E. R. Phenomenological Theory of Ion Solvation. Effective Radii of Hydrated Ions. *The Journal of Physical Chemistry* **63**, 1381-1387, doi:10.1021/j150579a011 (1959).

2 Smith, D. W. Ionic hydration enthalpies. *Journal of Chemical Education* **54**, 540, doi:10.1021/ed054p540 (1977).

3 Rong, Z. *et al.* Materials Design Rules for Multivalent Ion Mobility in Intercalation Structures. *Chemistry of Materials* **27**, 6016-6021, doi:10.1021/acs.chemmater.5b02342 (2015).

4 Ong, S. P. *et al.* Voltage, stability and diffusion barrier differences between sodium-ion and lithium-ion intercalation materials. *Energy Environ. Sci.* **4**, 3680-3688, doi:10.1039/c1ee01782a (2011).

5 Li, M. *et al.* Design strategies for nonaqueous multivalent-ion and monovalent-ion battery anodes. *Nature Reviews Materials* **5**, 276-294, doi:10.1038/s41578-019-0166-4 (2020).

6 Padhi, A. K., Nanjundaswamy, K. S. & Goodenough, J. B. Phospho-olivines as positive-electrode materials for rechargeable lithium batteries. *Journal of the Electrochemical Society* **144**, 1188-1194, doi:10.1149/1.1837571 (1997).

7 Ling, C., Banerjee, D., Song, W., Zhang, M. & Matsui, M. First-principles study of the magnesiation of olivines: redox reaction mechanism, electrochemical and thermodynamic properties. *Journal of Materials Chemistry* **22**, 13517-13523, doi:10.1039/C2JM31122D (2012).

8 Li, L. *et al.* Lithium Recovery from Aqueous Resources and Batteries: A Brief Review. *Johnson Matthey Technol. Rev.* **62**, 161-176 (2018).